Influence of the Addition of Aluminum in Boron-Doped Cz-Si on Degradation and Regeneration Kinetics

Melanie Mehler[1, a)], Andreas Schmid[1, b)], Annika Zuschlag[1, c)], Matthias Trempa[2, d)], Thomas Buck[3, e)], Giso Hahn[1, f)]

[1]*University of Konstanz, Department of Physics, D-78457 Konstanz, Germany*
[2]*Fraunhofer-Institute for Integrated Systems and Device Technology, D-91058 Erlangen, Germany*
[3]*International Solar Energy Research Center Konstanz e.V., Rudolf-Diesel-Straße 15, D-78467 Konstanz, Germany*

[a)] *Corresponding author: melanie.mehler@uni-konstanz.de*
[b)]*andreas.schmid@uni-konstanz.de*
[c)]*annika.zuschlag@uni-konstanz.de*
[d)]*matthias.trempa@iisb.fraunhofer.de*
[f)]*thomas.buck@isc-konstanz.de*
[e)]*giso.hahn@uni-konstanz.de*

Abstract. The impact of additional Al present in B-doped Cz-grown Si on the long-term behavior of excess charge carrier lifetime is investigated. From the resulting defect density and saturation current density j_0, after a degradation a delayed onset of regeneration and a delayed increase of the j_0 values can be observed in the material containing an order of magnitude more Al. The effect is less pronounced with constant injection as compared to constant generation conditions, but still significant and thus the causing effect seems to be injection-dependent. In addition to the time delay, a higher activation energy for the regeneration reaction can be determined. The effect of the delay could be shown not only for lifetime samples, but also for PERC solar cells. The developed model to explain the obtained findings is based on the assumption that due to the higher binding energy of Al-H pairs compared to B-H pairs, the release of H of the dopant-H complex is delayed and the regeneration reaction depends on this released H.

INTRODUCTION

Degradation phenomena, such as boron-oxygen related light induced degradation (BO-LID) and light and elevated temperature induced degradation (LeTID), have strong impact on the efficiency of Si solar cells by decreasing the charge carrier lifetime. Several factors such as firing temperature [1-3], gettering [4], and metal impurities [1,5,6] can influence the LeTID kinetics. Based on [7], the strength of LeTID degradation of Czochralski (Cz) PERC solar cells could be related to the aluminum concentration in the wafer. Therefore, Al could be involved in the responsible LeTID defect. In a previous work [8], the influence of Al on degradation and regeneration in lifetime samples was shown. The impact of Al dopants in the Si bulk on LeTID is additionally investigated here at the cell level. In order to shed light on the mechanism as well as the root cause behind LeTID on lifetime samples and on cell level, two comparable B-doped Cz-Si materials with different Al concentrations and its effects on degradation and regeneration kinetics are investigated in this work.

EXPERIMENTAL

B-doped and B+Al co-doped Cz-Si wafers (in the following referred to as "B-Reference" and "B+Al", respectively) serve as base material with a bulk resistivity of ~1 Ωcm. The Al concentration of B+Al ([Al]~$3\cdot10^{14}$ at/cm³) in the deliberately Al co-doped material is an order of magnitude higher than for the B-Reference

([Al]~4·10^13 at/cm³). For degradation experiments on wafer level, lifetime samples of size 5x5 cm² were used. After removal of the saw damage and a cleaning process, half of the samples receive a POCl₃-based emitter, which is removed in the next etching step ("gettered"). The other half of the samples did not receive a POCl₃-based emitter ("non-gettered"), but wafers are etched to the same thickness as the gettered ones, so that during firing the temperature-time profile is the same for all samples. After another cleaning process, SiN_y:H (75 nm) is deposited on both sides of all samples using direct plasma-enhanced chemical vapor deposition (PECVD). The samples are fired in a belt furnace at different firing temperatures, $T_{set,peak}$=750°C, 850°C or 900°C. The degradation treatment is carried out at 80°C, and either an illumination of 0.9(1) suns (constant generation) or constant injection [9] of $1·10^{16}$ cm⁻³ is used. The effective lifetime τ_{eff} is determined using photoconductance decay and evaluated at an excess charge carrier density of $\Delta n=0.1·p_0$, with p_0 being the doping density. For better comparison of the degradation and regeneration behaviour, the lifetime equivalent defect density ΔN_{leq} is calculated via

$$\Delta N_{leq}(t) = \frac{1}{\tau_{eff}(t)} - \frac{1}{\tau_{eff}(0)} \tag{1}$$

where $\tau_{eff}(0)$ and $\tau_{eff}(t)$ describe the effective lifetime directly after the final high-temperature step and at any time t, respectively [10]. In addition, saturation current density j_0 is determined according to [11,12] as a benchmark for surface passivation quality. The process flow of the lifetime samples is shown in Fig. 1 (a).

Full 6-inch Cz- and mc-PERC solar cells have been processed from both materials according to an industrial-type solar cell process to investigate degradation and regeneration on cell level. A schematic representation of the PERC solar cell structure is shown in Fig. 1 (b). The Al concentration in the B+Al mc-Si wafers ([Al]~2·10^14 at/cm³) is comparable to the Cz wafers and is also an order of magnitude higher compared to the B-Reference ([Al]~5·10^13 at/cm³) mc-Si wafer. The rear side of the cells is passivated with a silicon oxy-nitride layer SiO_xN_y and the front side with silicon nitride SiN_y:H. The solar cell parameters are determined using a flasher cetis PV from H.A.L.M. Since the initial open circuit voltage V_{OC} values of the cells are not the same, the difference ΔV_{OC} of the measured values to the initial value is considered for a better comparison.
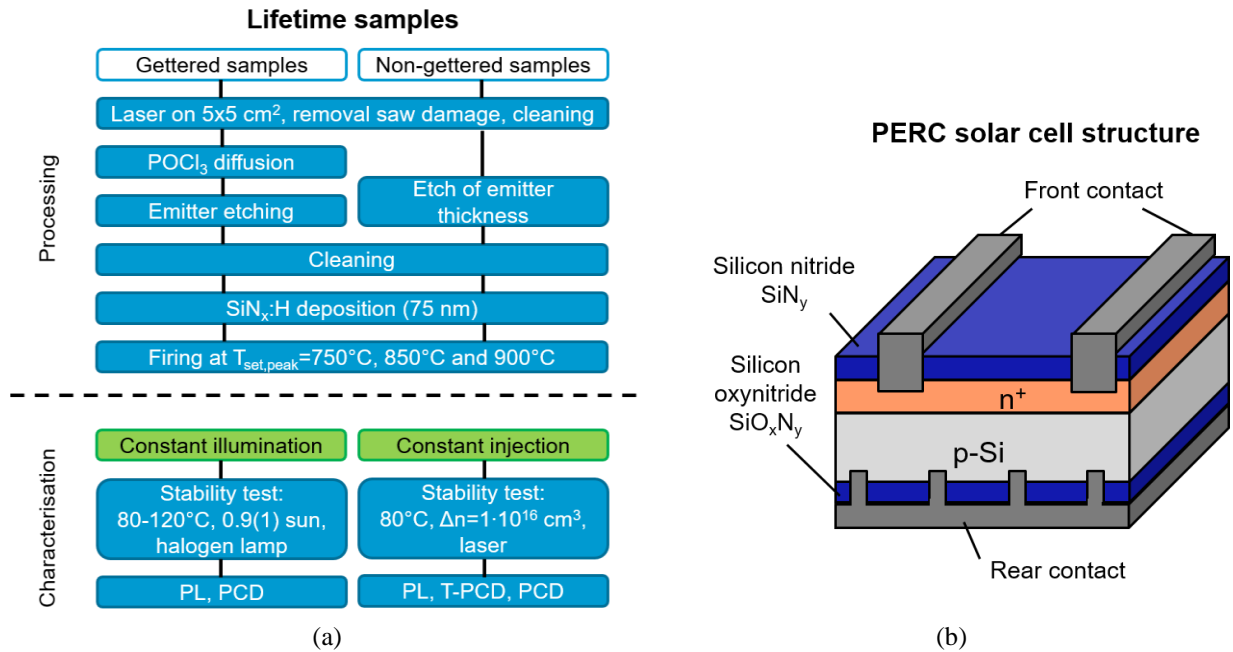

FIGURE 1. (a) Process diagram for the gettered and non-gettered lifetime samples. (b) Schematic representation of the PERC solar cell structure used here.

RESULTS

Constant Illumination – Cz-Si Lifetime Samples

Fig. 2 shows the resulting ΔN_{leq} and j_0 values for the two Cz-Si materials. By fitting ΔN_{leq}, the time constants for degradation and regeneration can be determined. According to [13] the degradation proceeds in two stages, a fast one followed by a slow degradation. For the fitting, two exponential functions for degradation and one exponential function for regeneration are used

$$\Delta N_{leq} = -a_1 exp\left(-\frac{t}{t_1}\right) - a_2 exp\left(-\frac{t}{t_2}\right) + a_3 exp\left(-\frac{t}{t_3}\right) + c \, , \tag{2}$$

with t_1 and t_2 the time constants of degradation, t_3 the time constant of regeneration, and c the offset.
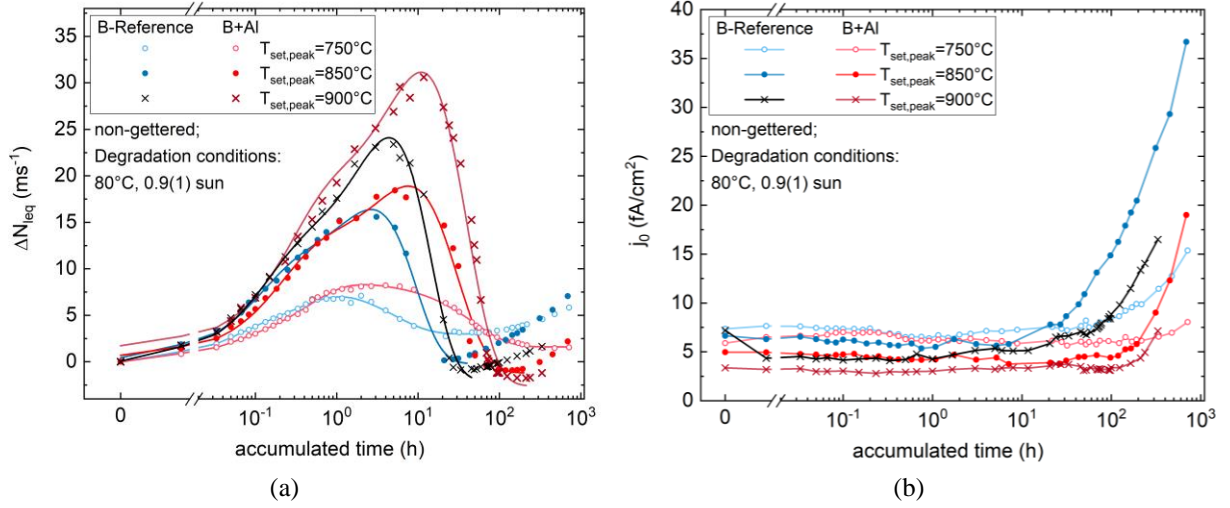

FIGURE 2. Defect density ΔN_{leq} with fit (a) and saturation current density j_0 (b), lines are guide to the eye, over accumulated time at constant illumination for non-gettered B-Reference and B+Al Cz-Si lifetime samples fired at different temperature. Some data are also shown in [8].

From the determined time constants, the corresponding rates can be determined via $r_x=1/t_x$, with x=1,2,3. The resulting rates are given in Tab. 1. The degradation of both materials is almost identical up to the ΔN_{leq}-maximum of the B-Reference. However, the onset of regeneration for the B+Al material is delayed compared to the B-Reference, as can be seen in Fig. 2 (a). Furthermore, the rates of regeneration r_3 for the B+Al samples are a factor of 4-13 lower than for the B-Reference and confirm the delay in regeneration compared to the B-Reference.

In addition to the defect densities, Fig. 2 (b) also shows a delayed increase of the j_0 values for the B+Al material. As an increase of j_0 is linked to a decrease of surface passivation quality, the addition of Al seems to have an influence on the surface degradation, too.

By comparing the gettered (not shown here) and non-gettered samples, it could also be shown that gettering has no significant effect on the degradation and regeneration behaviour.

Since the relative strength of BO-LID compared to LeTID decreases for higher firing temperatures [9], the lifetime measurements are done after firing steps with different peak temperatures. When comparing the rates r_3 of the regeneration, it is noticeable that the difference between the two materials becomes smaller at higher firing temperatures. Thus, a higher firing temperature reduces the Al-induced delay of regeneration for the B+Al material.

TABLE 1. Resulting rates for degradation (r_1, r_2) and regeneration (r_3) of the non-gettered B-Reference and B+Al Cz-Si samples by fitting the defect density ΔN_{leq} obtained at constant illumination and constant injection.

Treatment condition	Firing temperature	B-Reference	B+Al
Constant illumination	$T_{set,peak}$=750°C	r_1: 25(6) r_2: 4.35(19) r_3: 0.25(3)	r_1: 33(11) r_2: 2.63(7) r_3: 0.020(1)
Constant illumination	$T_{set,peak}$=850°C	r_1: 9.1(8) r_2: 0.37(11) r_3: 0.18(4)	r_1: 4.8(11) r_2: 0.17(3) r_3: 0.04(1)
Constant illumination	$T_{set,peak}$=900°C	r_1: 8.3(21) r_2: 0.23(9) r_3: 0.12(3)	r_1: 3.7(3) r_2: 0.11(3) r_3: 0.034(3)
Constant injection:	$T_{set,peak}$=850°C	r_1: 8,3(7) r_3: 0.91(1)	r_1: 7.7(6) r_3: 0.25(2)

In addition to considering the firing temperature on the degradation and regeneration kinetics, the activation energy for the non-gettered Cz-Si samples fired at 850°C and at degradation treatment temperatures of 80-120°C was determined. By using an Arrhenius plot, the activation energies E_A were determined from degradation and regeneration rates, see Fig. 3. While the determined activation energies for degradation are almost identical for B-Reference and B+Al, the activation energies of regeneration differ significantly for B-Reference ($E_{A,r3}$=0.77(5) eV) and B+Al ($E_{A,r3}$=1.03(14) eV).
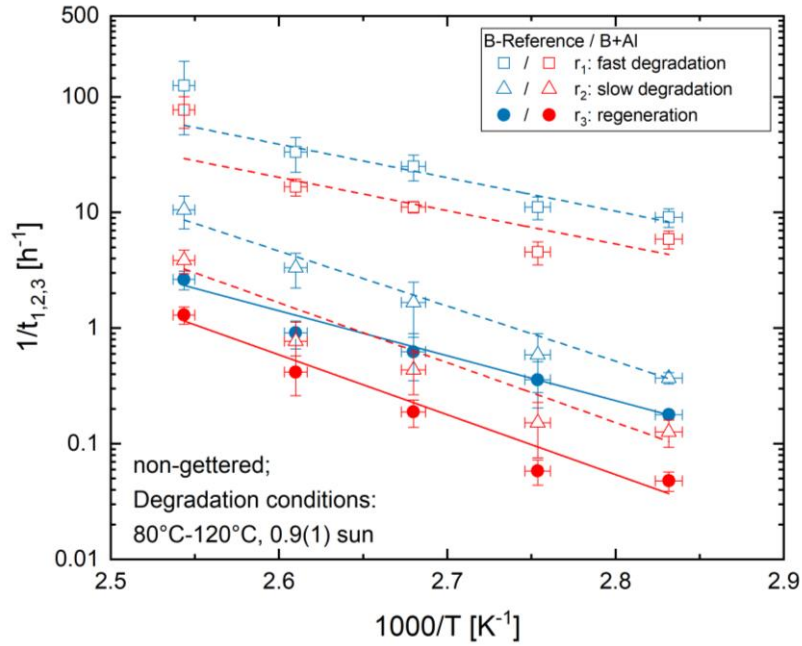

FIGURE 3. Temperature-dependent degradation and regeneration rates of B-Reference (black) and B+Al (red) with associated Arrhenius fit.

Constant Injection – Cz-Si Lifetime Samples

Since τ_{eff} changes over time, injection also changes and this might change the (injection-dependent) reaction rates [9,14]. Therefore, the experiment was repeated under constant injection conditions ($\sim 1 \cdot 10^{16}$ cm^{-3}). The resulting defect densities ΔN_{leq} and j_0 values are shown in Fig. 4. Degradation kinetics have now changed compared to the first investigation, and only one exponential function is sufficient to fit the degradation phase with very good accuracy. The difference of rates for regeneration is smaller at constant injection (factor of 2-4) as compared to constant illumination conditions (factor of 4-5) (*cf.* Tab. 1). Since the delay of regeneration at constant injection for B+Al fired at $T_{set,peak}$=850°C is less pronounced compared to constant illumination, but still significant, the underlying mechanism seems to be injection dependent.
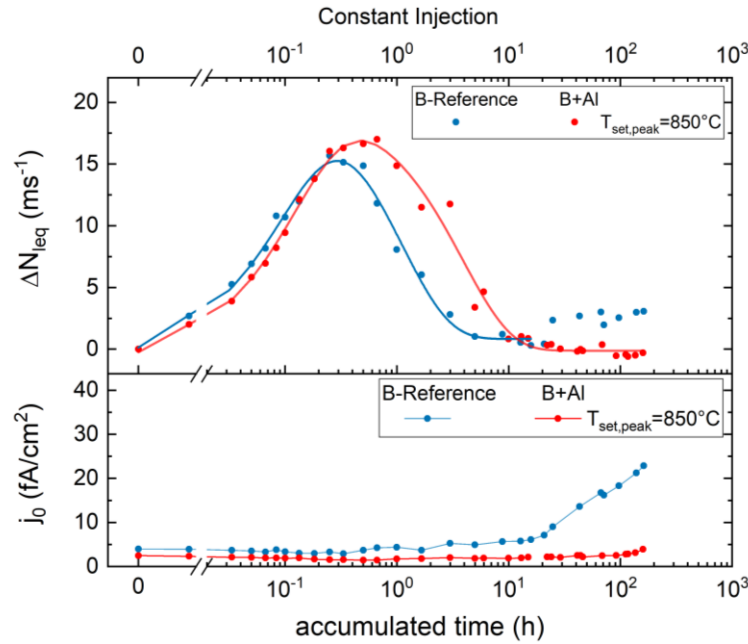

FIGURE 4. Defect density ΔN_{leq} with fit and j_0 (lines are guide to the eye) over accumulated time at constant injection for non-gettered B-Reference and B+Al Cz-Si lifetime samples fired at (a) 850°C. Data are also shown in [8].

Degradation and regeneration kinetics of Cz and mc-PERC solar cells

The influence of the addition of Al on degradation and regeneration kinetics was investigated at solar cell level at 80°C and 0.9(1) sun (analogous to the lifetime samples at constant generation). Fig. 5 shows the ΔV_{oc} values of the two Cz-Si PERC cells. The progression of the ΔV_{oc} values show a degradation and a regeneration, and the renewed observed decrease in ΔV_{oc} for longer times (>100-200 h) is most likely caused by a decrease in surface passivation quality. It can be seen that the degradation behaviors are almost identical up to the degradation maximum of the B-Reference. It can also be seen, that the addition of Al leads to a delay in regeneration, which is consistent with the observations on wafer level as discussed above. The same qualitative behavior was also observed for mc-PERC solar cells (not showed).
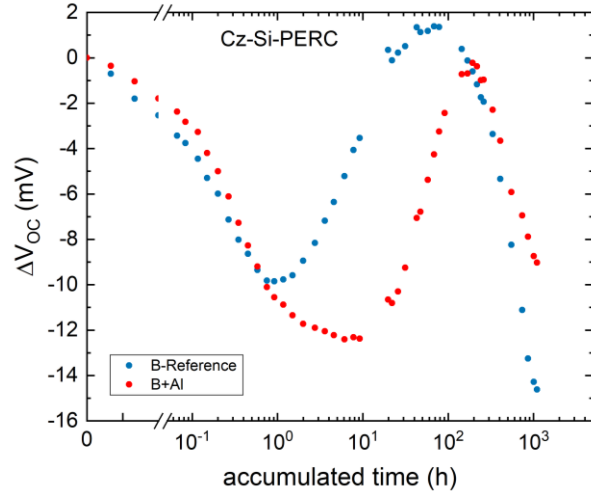
FIGURE 5. ΔV_{oc} values of the Cz-PERC solar cells from the two base materials B-Reference and the B+Al over accumulated time at 80°C, 0.9 sun illumination.

DISCUSSION

Since the B concentration (~$1\cdot10^{16}$ at/cm^3) is nearly the same in both materials, the differences in ΔN_{leq} behavior most probably originate from the Al concentration. LeTID is more pronounced compared to BO-LID at higher firing temperatures. However, since the delay in regeneration occurs at all firing temperatures considered, Al seems to slow down the BO and/or LeTID regeneration process. Possible causes for the delay could therefore be the dopant itself and its influence on the possible binding partners, such as H, which seems to play an important role in the LeTID defect [2] as well as the BO-regeneration [15]. The binding energy in the dark for Al-H of E_b=1.44±0.03 eV is higher than for B-H (1.28±0.03 eV) [16]. Thus, the release of H from Al-H could also be slower under injection. Assuming that the regeneration depends on this released H from the complex, this might explain the delay in the lifetime samples and also in the cells. As also a delay in the onset of decrease of surface passivation quality is observed in the B+Al lifetime samples (j_0), this decrease might be caused by H (freed from the dopant) diffusing towards the surface.

CONCLUSION

Addition of Al leads to a time delay in regeneration and might have an influence on surface degradation. Since LeTID dominates over BO-LID at higher firing temperatures, different firing temperatures were considered. It could be shown that a higher firing temperature delays the Al-induced delay in regeneration, but the effect is still significant. Thus, because the effect of the delay cannot be clearly attributed to BO-LID or LeTID, Al seems to slow down BO-LID and/or the LeTID regeneration process. When determining the activation energy, a higher activation energy for regeneration could be defined for B+Al. In the investigation with constant injection, the delay is not as pronounced as for constant illumination, but is still significant. Also, compared to constant illumination, one exponential function was sufficient to fit the degradation. Thus, the effect seems to depend on injection. In addition to the lifetime samples, the delay in regeneration could also be observed at cell level for Cz-Si and mc-Si PERC cells.

ACKNOWLEDGMENTS

REFERENCES

1. D. Bredemeier, D. Walter, S. Herlufsen, J. Schmidt, AIP Advances **6**(3), 035119 (2016).
2. R. Eberle, W. Kwapil, F. Schindler, M. C. Schubert, S. W. Glunz, Phys. Status Solidi RRL **10**, 861-865 (2016).
3. D. Skorka, A. Zuschlag, G. Hahn, AIP Conference Proceedings **1999**, 130015 (2018).
4. D. Bredemeier, D. C. Walter, J. Schmidt, Solar RRL 2(1), 1700159 (2018).
5. K. Nakayashiki, J. Hofstetter, A. E. Morishige, T.-T. A. Li, D. B. Needleman, M. A. Jensen, T. Buonassisi, IEEE J. Photovolt. **6**(4), 860-868 (2016).
6. M. A. Jensen, A. E. Morishige, J. Hofstetter, D. B. Needleman, T. Buonassisi, IEEE J. Photovolt. **7**(4), 980-987 (2017).
7. M. Wagner, F. Wolny, M. Hentsche, A. Krause, L. Sylla, F. Kropfgans, M. Ernst, R. Zierer, P. Bönisch, P. Müller, N. Schmidt, V. Osinniy, H.-P. Hartmann, R. Mehnert, H. Neuhaus, Sol. Energy Mater. Sol. Cells **187**, 176-188 (2018).
8. M. Mehler, A. Schmid, A. Zuschlag, M. Trempa, G. Hahn, Phys. Status Solidi A, **218**(22), 2100603 (2021).
9. A. Graf, A. Herguth, G. Hahn, AIP Conference Proceedings, **2147**, 140003 (2019).
10. A. Herguth, IEEE J. Photovolt. **9**(5), 1182-1194 (2019).
11. A. Kimmerle, J. Greulich, A. Wolf, Sol. Energy Mater. Sol. Cells, **142**, 116 (2015)
12. D. E. Kane and R. M. Swanson, "Measurement of the emitter saturation current by a contactless photoconductivity decay method," in *Conf. Record 18th IEEE PVSC* (1985), pp. 578-583.
13. D. Bredemeier, D. Walter, J. Schmidt, Sol. Energy Mater. Sol. Cells. Cells **173**, 2-5 (2017).
14. D. C. Walter, L. Helmich, D. Bredemeier, R. Falster, V. V. Voronkov, J. Schmidt, "Lifetime evolution during regeneration in boron-doped Czochralski-Silicon," in *Proc. 35th EUPVSC* (2018), pp. 522-526.
15. S. Wilking, A. Herguth, G. Hahn, Journal of Applied Physics, **113**(19), 194503 (2013).
16. T. Zundel and J. Weber, Phys. Rev. B **39**, 13549 (1989).